The Free Internet Journal for Organic Chemistry

Paper

Archive for Organic Chemistry

Arkivoc **2020**, part ii, 53-60

Characterization of organic isomers: CID fragmentation technique on protonated hydroxybenzophenone isomers

Juan Z. Dávalos*[a], Luis R. Carlos[b], Héctor R. Loro,[b] and Alexsandre F. Lago*[c]

[a] *Instituto de Química Física Rocasolano, CSIC. c/Serrano, 119.E-28006 Madrid, Spain*

[b] *Facultad de Ciencias, Universidad Nacional de Ingeniería, Av. Túpac Amaru 210 - Rímac. Apartado 1301, Lima, Peru*

[c] *Centro de Ciências Naturais e Humanas, Universidade Federal do ABC (UFABC), Av. Dos Estados, 5001, 09210-580, Santo André, SP, Brazil*

E-mails: jdavalos@iqfr.csic.es, alexsandre.lago@ufabc.edu.br

This manuscript is dedicated to Prof. José M. Riveros

Received 11-01-2019 **Accepted** 01-27-2020 **Published on line** 02-10-2020

Abstract

We have studied the fragmentation dynamics of the protonated 2-, 3- and 4-hydroxybenzophenones (**2**H^+, **3**H^+ and **4**H^+, 191 *m/z*) obtained by CID ("Collision Induced Dissociation") technique coupled to Mass Spectrometer with electrospray source (MS-ESI). The CID-fragmentation patterns involve the $C_7OH_5^+$ (105 *m/z*) and $C_7O_2H_5^+$ (121 *m/z*) cations, for which the intensity ratio is typical to the isomer considered. **2**H^+ and **3**H^+ yield preferably $C_7O_2H_5^+$ (121 *m/z*) and $C_7OH_5^+$ (105 *m/z*) respectively, while **4**H^+ yields both cations in similar quantity. The fragmentation pathways were analyzed and discussed, taking into account the "model of free-proton" and results from computational calculations at B3LYP/6-311++G(d,p) level of theory.

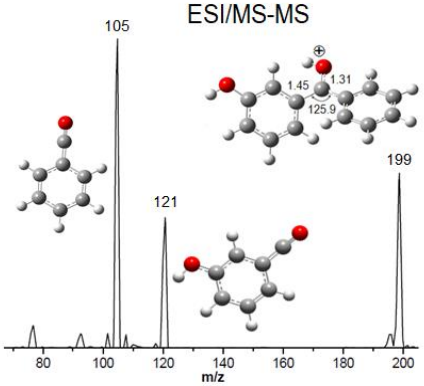

CID/MS-ESI fragmentation technique employed to characterize hydroxybenzophenone isomers. Main structures in the spectrum: Parent cation (199 *m/z*), $C_7O_2H_5^+$ (121 *m/z*), $C_7OH_5^+$ (105 *m/z*).

Keywords: Isomers, hydroxybenzophenone, protonation, fragmentation, ESI-MS, CID, DFT calculations

Introduction

Protonation is a common occurring process within chemical and biological systems,[1] which usually results in the formation of hydrogen bonds.[2] Several studies have been carried out to determine the preferred site of protonation from small molecules, such as carbon monoxide,[3] up to large ones, such as proteins and peptides.[4] In those systems, it has been found that the proton tends to attach to a thermodynamic favourable site that gives rise to a stable mono-charged cation (z = +1). However, in some cases, such as biological molecules, there might be different preferred sites of protonation (multi-protonated, z = +n) which indicates that protonation may be regarded as a competitive process between the thermodynamical and kinetical natures.[5] Mass spectrometry is acknowledged as a powerful analytical technique which allows processes such as ionization/protonation/deprotonation/fragmentation in order to identify specific molecules and their products, and it may also be coupled with other complementary techniques, (e.g. CID) to conduct further structural analysis.

Typically, protonation takes place when the proton migrates from its preferred site to another region within the molecule. As an example, the protonation of the amide has been shown to occur at the oxygen located in the carbonyl group C=O,[6] but the fragmentation only takes place when the proton migrates to the nitrogen in the amide group, despite the fact that the N- protonated species might have higher energies than the O-protonates isomers.[7] Since the previous process is a recurrent behaviour in many molecules, it has led to the proposition of the "mobile proton model" [8,9] to describe the mobility of the proton through protonated molecules.

In this research, it has been studied the fragmentation of protonated 2-, 3- and 4- hydroxybenzophenones (**2**H^+, **3**H^+ and **4**H^+) using CID technique ("Collision Induced Dissociation") along with a triple quadrupole mass spectrometer (MS-TQ) coupled with electrospray source (MS-ESI). The experimental results have been analysed and rationalized by means of the density functional theory (DFT) computational calculations, performed at the B3LYP/6-311++G(d,p) level of theory. It is important to point out that CID fragmentation mass spectrometry experiments are very effective in the identification of chemical species. In this study, we have shown that through these techniques the isomer species could be unequivocally identified.

Results and Discussion

The Hydroxybenzophenones isomer species were protonated on their carbonyl groups C=O [10] and identified by the peak at 199.1 *m/z* (parent cation) in the mass spectrum. The CID fragmentation of these cations produced two fragments, identified as the 105 and 121 *m/z* peaks in the mass spectra (Figure 1), for which the relative intensities increase as the dissociation energy rises, while the intensity of parent cation decreases.

The previous result indicates the existence of two competitive channels of CID fragmentation, as described in the proposed mechanisms in Figure 2. In the first dissociation channel (I) it is produced a $C_7OH_5^+$ cation (105 *m/z*) and a neutral phenol molecule; and in the second channel (II) it is produced a $C_7O_2H_5^+$ (121 *m/z*) cation and a neutral benzene molecule. The proportion of intensities of the peaks associated with these cations produce a CID pattern, which characterizes the fragmentation of these isomers (Figure 3).

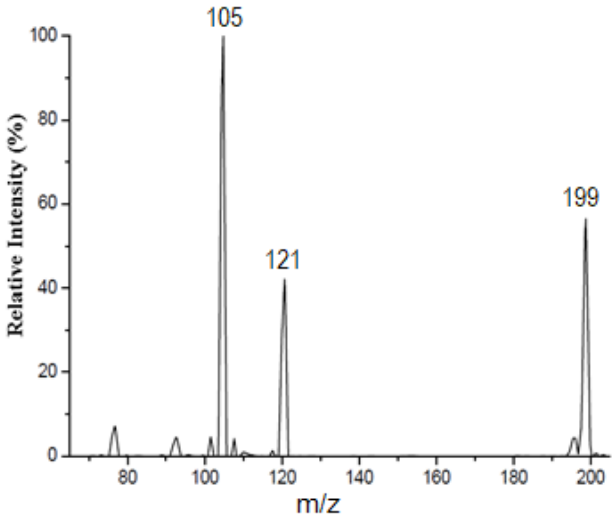

Figure 1. Typical mass spectrum of **3**H$^+$ isomer, fragmented at the energy E_{cm} = 3.35 eV.

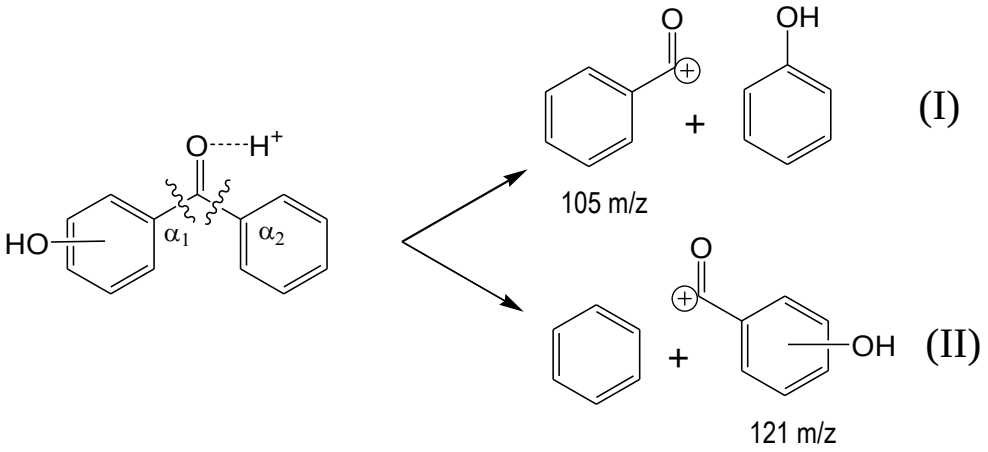

Figure 2. Fragmentation diagram of hydroxybenzophenone isomers.

According to the proton mobile model, it is noticeable that depending on in which of the carbon atoms the fragmentation takes place, $C_{\alpha 1}$ or $C_{\alpha 2}$ on the benzene rings, the proton could migrate. It would lead to one of the two proposed fragmentation mechanisms. It is interesting to point out for the CID experiments involving the **2**H$^+$, **3**H$^+$ and **4**H$^+$ protonated-hydroxybenzophenones, that by varying the energy E_{cm} the formation of both fragments (at 105 and 121 *m/z*), with rates of formation (I_{105}^+/I_{121}^+), were mostly independent of E_{cm} (Figure3). The fragmentation route (II) is preferable in the fragmentation of **2**H$^+$ isomers, meanwhile the route (I) is followed by **3**H$^+$ species. In the case of **4**H$^+$ isomers, both routes have roughly the same probability.

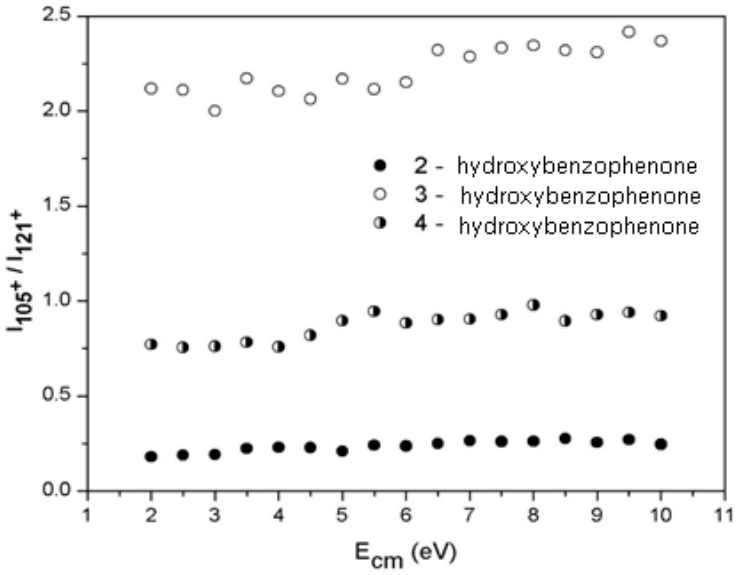

Figure 3. CID fragmentation pattern of 2-, 3- and 4- protonated hydroxybenzophenone isomers.

Energetic analysis of fragmentation

The optimized geometries, obtained at B3LYP/6-311++G(d,p) level of theory, of the most stable hydroxybenzophenone-protonated rotamers, $\mathbf{2}_a\mathrm{H}^+$, $\mathbf{3}_a\mathrm{H}^+$ and $\mathbf{4}_a\mathrm{H}^+$ are presented in Figure 4, for which the populations were 99.9%, 29% and 51%, respectively. It is important to notice that the proton in $\mathbf{2}_a\mathrm{H}^+$ forms a hydrogen bonding with the phenol part in its molecule, this feature seems to prevent the proton from behaving as a "free-proton" and thus influencing the fragmentation mechanism. On the contrary, for the $\mathbf{3}\mathrm{H}^+$ and $\mathbf{4}\mathrm{H}^+$ rotamers (and also other $\mathbf{2}\mathrm{H}^+$ rotamers) that particularity was not observed.

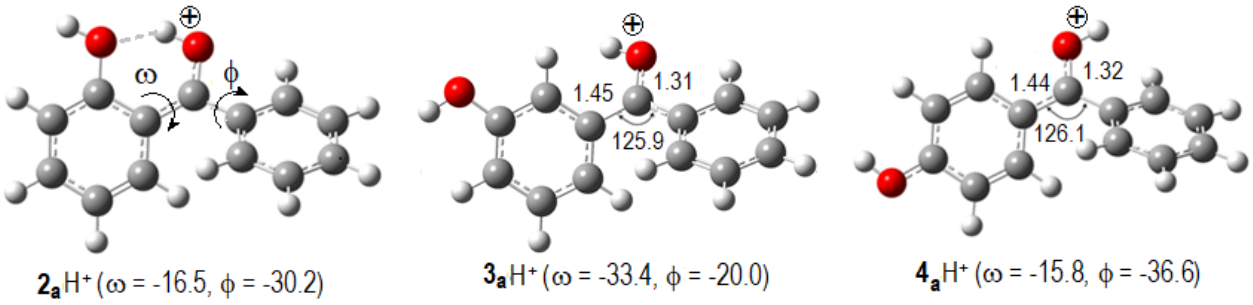

Figure 4. Optimized geometries, at B3lYP/6-311++G(d,p) level, of the most stable rotamers of $\mathbf{2}\mathrm{H}^+$, $\mathbf{3}\mathrm{H}^+$ and $\mathbf{4}\mathrm{H}^+$ hydroxybenzophenones. Angles and distances are given in degrees and Å, respectively.

Fragmentation of $\mathbf{2H^+}$: In Figure 5, distinct fragmentation pathways possible for the $\mathbf{2}\mathrm{H}^+$ are shown. The proton on the most stable rotamer $\mathbf{2}_a\mathrm{H}^+$ is oriented towards $C_{1\alpha}$ (phenolic group), but its fragmentation following the route (I) would have to overcome a high energy barrier with a transition state TS_{1a} of 327.3 kJ·mol^{-1} . This barrier should be increased by the presence of a hydrogen bonding, as previously described. Consequently, the direct fragmentation of $\mathbf{2}_a\mathrm{H}^+$ is diminished in favour of the formation of the other rotamers such as $\mathbf{2}_b\mathrm{H}^+$ or $\mathbf{2}_f\mathrm{H}^+$, overpassing much smaller barriers ($TS_{i\text{-}k}$ between 12 and 58 kJ·mol^{-1}). Considering that $\mathbf{2}_a\mathrm{H}^+$ is subjected to this isomerization process with a population rebalancing, the rotamers with "free-

protons" oriented towards $C_{1\alpha}$, which will follow the fragmentation route (I), accounted for approximately 15% of the conformational population. The proportion of these species to those which will follow the route (II) has been found to be *r* = 0.18, a consistent value, comparable with the experiments (Figure 3).

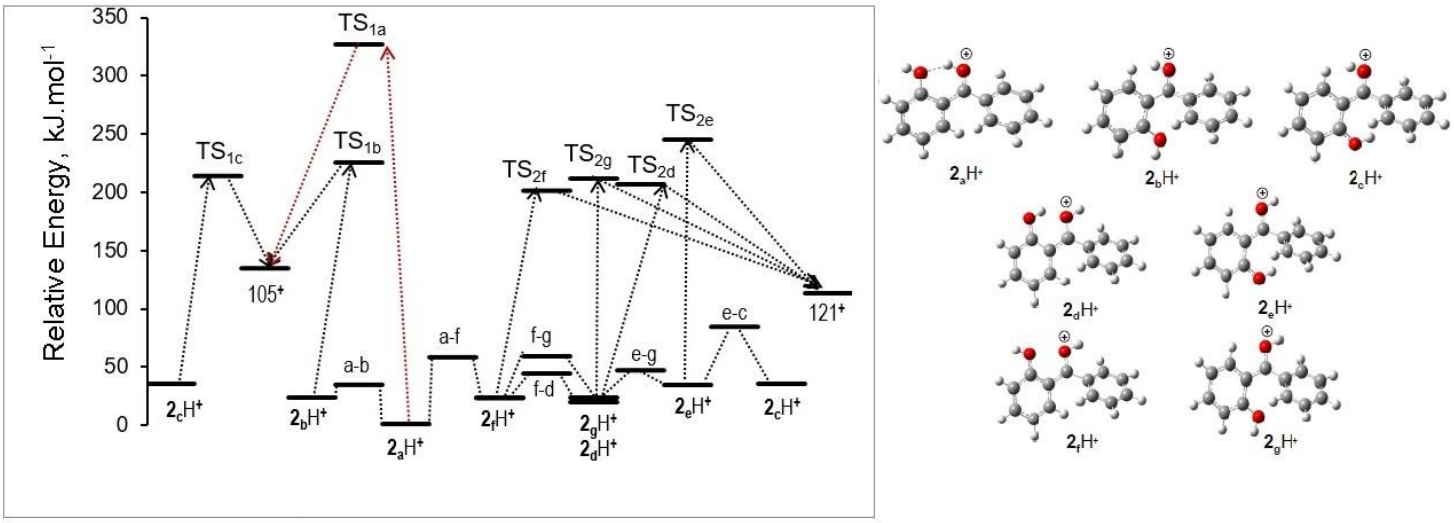

Figure 5. Energy diagram showing the routes of fragmentation of $\mathbf{2}_k H^+$ rotamers (k = a, b, …, g). Transition states: (i-k) of rotamers from $\mathbf{2}_i H^+$ to $\mathbf{2}_k H^+$; TS_{nk} (n = 1, 2).

Fragmentation of 3H$^+$ (Figure 6)**:** $\mathbf{3}H^+$ rotamers (including the most stable, $\mathbf{3}_a H^+$) with the proton oriented against $C_{\alpha 1}$ represented 65.5% of the conformational population, and considering their "free-protons" character, these species tend to follow the fragmentation route (I) , overcoming energy barriers with TS_{1k} between 172 and 177 kJ·mol^{-1}.

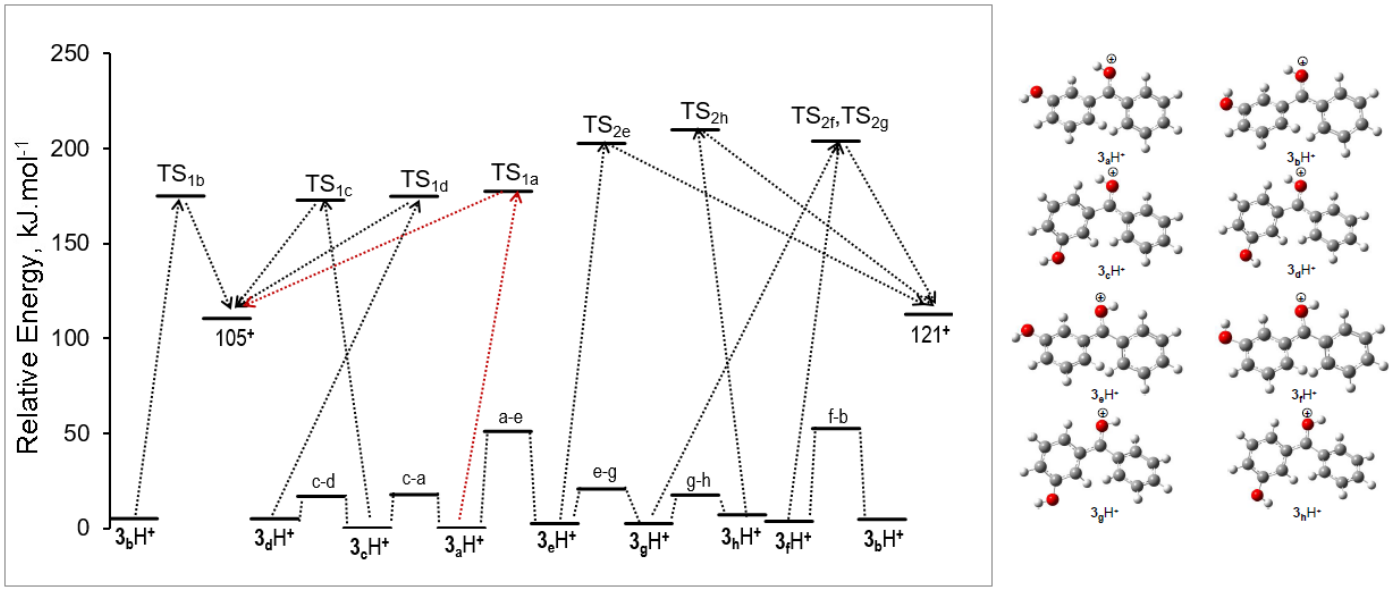

Figure 6. Energy diagram showing routes of fragmentation of $\mathbf{3}_k H^+$ rotamers (k = a, b, …, g). Transition states: (i-k) of rotamers from $\mathbf{3}_i H^+$ to $\mathbf{3}_k H^+$; TS_{nk} (n = 1, 2).

Rotamers with the proton oriented towards $C_{\alpha 2}$ (benzene group) represented a population of 34.5% and should follow the route (II) overpassing barriers with TS_{2k} between 200 and 203 kJ·mol^{-1} kJ·mol^{-1}. It is easy to appreciate that the rotamers which fragment following the route (I) accounts for almost the double, proportionally, as compared to those which follow route (II), and they should be favoured by the fact that they have to overcome barriers of about 30 kJ·mol^{-1} lower in energy than by following route (I). This proportion, as described before, is in good agreement with the experimental results (Figure 3).

Fragmentation of 4H$^+$ (Figure 7): **4$_a$**H$^+$ and **4$_b$**H$^+$ rotamers, with the proton oriented towards $C_{\alpha 2}$, accounted for 91.5% of the conformational population. These species also behave as "free-protons" and should also tend to follow the fragmentation route (II), overcoming energy barriers with TS_{2k} of approximately 207 kJ·mol^{-1}. **4$_c$**H$^+$ and **4$_d$**H$^+$ rotamers, with the proton oriented towards $C_{\alpha 1}$, tend to follow route (I). Although these species only represent 8.5% of the population, their populations should increase at the expense of the most abundant ones (**4$_a$**H$^+$ and **4$_b$**H$^+$). This is due to the barriers TS_{2k} that they should surpass, which are almost 16 kJ·mol^{-1} less energetic than TS_{1k}.

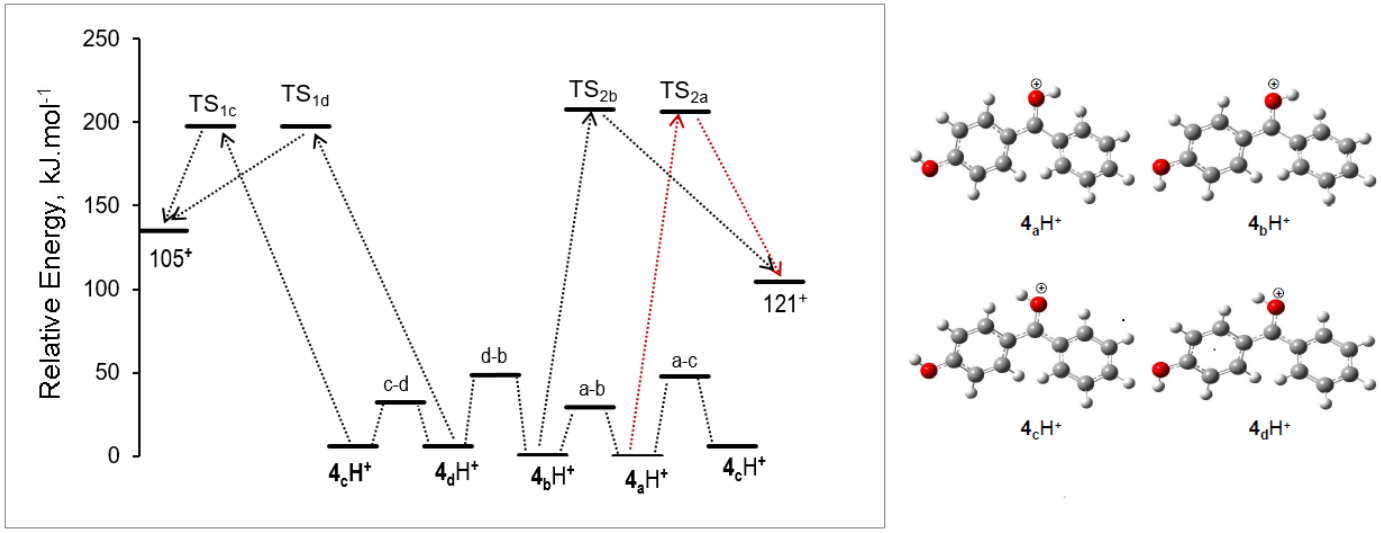

Figure 7. Energy diagram showing routes of fragmentation of **4$_k$**H$^+$ rotamers (k = a, b, …, g). Transition states: (i-k) of rotamers from **4$_i$**H$^+$ to **4$_k$**H$^+$; TS_{nk} (n = 1, 2).

Conclusions

The analysis of the results of the CID fragmentation of protonated hydroxybenzophenone isomers, through the construction of characteristic fragmentation patterns, has allowed the unequivocal identification of these isomers, and to determine their relative populations. The fragmentation mechanisms were studied and analysed using DFT computational calculations, in conjunction with general scientific concepts, such as "mobile proton model", transition states, and conformational populations, which were useful for the prediction of the most favourable routes. From this approach, we have found that the **2**H$^+$ isomers tend to fragment preferably following the route that leads to the formation of the $C_7O_2H_5^+$ (121 *m/z*) cation. On the contrary, the **3**H$^+$ isomers preferably form the $C_7OH_5^+$ cation (105 *m/z*), and the **4**H$^+$ species fragment forming cations in similar proportions. The results obtained at B3LYP/6-311++G(d,p) level of theory were satisfactory to support the explanations of the fragmention pathways involving the hydroxybenzophenone isomers.

Experimental Section

General. The experiments were carried out on a triple quadrupole mass spectrometer (Varian 320) equipped with an electrospray ionization (ESI) source. For each isomer, we prepared solutions of $5x10^{-5}$ M in a mix of acetonitrile/water dissolvent (1:1), by adding small quantities of acetic acid (approximately 2 μL per 1 of mL of dissolution) in order to promote protonation. These solutions were directly infused into the ESI ionization source at flow rates between 10-20 μL/min. Capillary voltages and other parameters were adjusted to maximize the intensity of cations of interest. The cations produced were isolated in the first quadrupole (Q1), underwent collision induced dissociation (CID) in the second quadrupole (Q2), and the resulting fragments were analysed in the third quadrupole (Q3). CID experiments were performed using argon as the collision gas (0.8 mTorr), at various ion kinetic energies in the collision cell so that the centre of mass energy (E_{cm}) took values from 2 to 10 eV. The final rate of produced fragments represented an average on 200 confident measurements.

Materials. 2-, 3- and 4- Hydroxybenzophenones ($C_{13}H_{10}O_2$, which we denote respectively as **2**, **3** and **4**) were obtained from Sigma Aldrich and used without further purification.

Computational details. The quantum chemical calculations were carried out using the Gaussian 09 package.[11] The geometries of all the studied species were optimized by using density functional theory (DFT), with the Becke 3-parameter and Lee-Yang-Parr (B3LYP)[12,13] functional, in conjunction with a 6-311++G(d,p) basis set, without symmetry restrictions. Harmonic vibrational frequencies were also calculated at the same level and used without scaling. The transition states (TS) structures were optimized using QST2 methodology,[14] in which each of these structures connect the reactants with the corresponding products. TS´s were characterized by the presence of an imaginary frequency. The theory methods used in this research are widely used in quantum chemical applications and were considered suitable by providing consistent and comparable results with experimental measurements.[15-17]

Acknowledgements

This research has been possible thanks to the support of the scholarship program UNI-agreement N◦ 167 - 2015 - Fondecyct UNI Consejo Nacional de Ciencia, Tecnología e Innovación Tecnológica, CONCYTEC. A special thanks to Rocío Ramos (JAE-tec) from laboratory of Thermochemistry of IQFR-CSIC, Madrid. A.F.L. acknowledges the support from the brazilian funding agencies: Conselho Nacional de Desenvolvimento Científico e Tecnológico (CNPq), Coordenação de Aperfeiçoamento de Pessoal de Nível Superior (CAPES), Fundação de Amparo à Pesquisa do Estado de São Paulo (FAPESP).

Supplementary Material

Optimized geometries, at the B3LYP/6-311++G(d,p) level of theory, for the **2**H^+, **3**H^+ and **4**H^+ rotamers, and also for the fragments of 105 and 121 *m/z*, are given in the supplementary material associated with this manuscript.

References

1. Scheiner, S. *Acc. Chem. Res*. **1985**, *18*, 174-180. https://doi.org/10.1021/ar00114a003
2. Chan, B.; Del Bene, J.; Elguero, J.; Radom, L. *J. Phys. Chem*. A **2005**, *109*, 5509-5517. https://doi.org/10.1021/jp0516994
3. Jansen, B.; Ros, P. *Theor. Chim. Acta* **1971**, *21*, 199-204. https://doi.org/10.1007/BF00530218
4. Cox, K. A.; Gaskell, S. J., Morris, M.; Whitting, A. *J. Am. Soc. Mass Spectrom*. **1996**, *6*, 522-531. https://doi.org/10.1016/1044-0305(96)00066-9
5. Weisz, A.; Cojocaru, M.; Mandelbaum. A. *J. Chem. Soc., Chem. Commun.* **1989**, *6*, 331-332. https://doi.org/10.1039/c39890000331
6. Perrin, C. L. *Acc. Chem. Res*. **1989**, *22*, 268-275. https://doi.org/10.1021/ar00164a002
7. Lin, H.; Ridge, D. P.; Uggerud, E.; Vulpius, T. *J. Am. Chem. Soc*. **1994,** *116*, 2996-3004. https://doi.org/10.1021/ja00086a032
8. Mueller, D. R.; Eckersley, M.; Richter, W. *Org. Mass. Spectrom*. **1988**, *23*, 217-222. https://doi.org/10.1002/oms.1210230312
9. Csonka, I. P.; Paizs, B.; Lendvay, G.; Suhai, S. *Rapid Commun. Mass. Spectrom*. **2000**, *14*, 417-431. https://doi.org/10.1002/(SICI)1097-0231(20000331)14:6<417::AID-RCM885>3.0.CO;2-J
10. Benoit, F. M.; Harrison, A. G. *J. Am. Chem. Soc*. **1977**, *99*, 3980-3984. https://doi.org/10.1021/ja00454a015
11. Frisch, M. J. *et al. Gaussian 09*, Revision A.01 Wallingford CT, 2009.
12. Becke, A.D. *J. Chem. Phys*. **1993**, *98*, 5648-5652. https://doi.org/10.1063/1.464913
13. Lee, C.; Yang, W.; Parr, R.G. *Phys. Rev. B* **1988**, *37*, 785-789. https://doi.org/10.1103/PhysRevB.37.785
14. Jensen, A. *Theor. Chem. Acc*. **1983**, *63*, 269-290. https://doi.org/10.1007/BF01151605
15. Raghavachari, K.; Stefanov, B. B.; Curtiss, L.A. *Mol. Phys*. **1997**, *91*, 555-560. https://doi.org/10.1080/002689797171445
16. Hehre, W.J.; Radom, L.; Schleyer, P.v.R.; Pople, J.A. *Ab initio Molecular Orbital Theory*, John Wiley & Sons, New York, 1986.
17. Sivaranakrishnan, R.; Tranter, R.S.; Brezinsky, K. *J. Phys. Chem. A*, **2005**, *109*, 1621-1628. https://doi.org/10.1021/jp045076m